Preliminary Study on Single-phase Natural Circulation under Dynamic Motions in MARS-KS Code

Ju Hun Jung, In Cheol Bang*

Dept. of Nuclear Engr., Ulsan National Institute of Science and Technology (UNIST).,
50 UNIST-gil., Ulju-gun., Ulsan., Republic of Korea
*Corresponding author: icbang@unist.ac.kr

1. Introduction

Since the ultimate goal is zero-emission from the ship operation and the regulation on green house gas (GHG) emissions will be continuously strengthened, ship-building industries are regarding nuclear energy as the next generation propulsion of the ships. Hence, as interest in floating nuclear power plants (FNPPs) and nuclear propulsion ships increases, various FNPPs prototypes worldwide have been developed [1].

Natural circulation could be characterized due to its own passive safety, which is based on buoyancy as a driving force using gravity due to the difference in the density of the working fluid depending on the temperature change. Thus, the application of natural circulation to offshore reactors is sufficiently reasonable as maritime reactors generally have more difficulty than land-based reactors owing to the periodical and dynamic motions in ocean environments. However, natural circulation is considerably affected by external forces since the driving force of natural circulation decreases more than that of forced circulation [2].

Above all, the marine reactors should adopt SMR designs since they need compact size and a high volumetric heat generation rate due to the limit on size. Several SMR designs, especially Gen-IV liquid metal-based reactors (LMRs) and Gen-III+ small light water-based reactors, are being considered candidates for FNPPs and ship propulsion reactors.

Small pressurized water reactors (PWRs) design has some advantages of a sufficient supply of coolant, various experimental experiences, and several practical operating cases. However, the disadvantages of the high operating pressure and coolant boiling probability also exist.

LMRs have several attractive benefits as marine reactors. Representatively, LMRs could have a passive safety due to the natural solidification of coolant when the reactor tripped, or a severe accident occurred. Moreover, nuclear fuel replacement cannot be necessary because a long fuel cycle would match the life of the ship. LMRs could ease to reduce the reactor size due to high thermal efficiency. Nevertheless, further research is needed on several reactors including LMRs as candidates for marine reactors since there are few numbers of experiments and studies.

Therefore, thermal-hydraulic analysis of LMRs, which are being developed for the maritime reactors in Korea, was additionally carried out to obtain the fundamental safety analysis data. The numerical analysis was conducted for the thermal-hydraulic natural circulation phenomena in a simple test loop under the dynamic motions by a numerical analysis code. The simulation results were interpreted according to each motion type or working fluid, light water, and lead-bismuth eutectic (LBE).

2. Mathematical Governing Equation

Three-dimensional motions caused by oceanic environments, such as tides, winds, and waves, affect offshore structures. These are including three translational motions and three rotational motions, which are called six degrees of freedom [3].
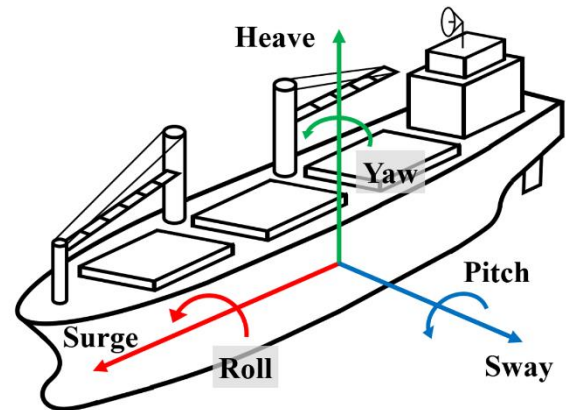

Fig. 1. Six degrees of freedom in ship.

Acceleration, which is representing six degrees of freedom as well as gravity, includes rotational acceleration and linear acceleration. Acceleration can be written the mathematical form [4] in the momentum equation as,

$$\rho \left(\frac{\partial \boldsymbol{u}}{\partial t} + \boldsymbol{u} \cdot \nabla \boldsymbol{u} \right) = -\nabla p + \nabla \cdot \boldsymbol{\tau} + \rho \boldsymbol{g}$$
$$- \rho \left[\frac{d^2 \boldsymbol{R}}{dt^2} + \boldsymbol{\Omega} \times (\boldsymbol{\Omega} \times \boldsymbol{r}) \right. \quad (1)$$
$$\left. + 2\boldsymbol{\Omega} \times \boldsymbol{u} + \frac{D\boldsymbol{\Omega}}{Dt} \times \boldsymbol{r} \right]$$

where, ρ, $\boldsymbol{u}$, p, $\boldsymbol{\tau}$, $\boldsymbol{g}$ is density, fluid velocity, pressure, shear stress, and gravitational acceleration, respectively. Four fictitious accelerations are contained in Eq. (1). $\boldsymbol{R}$ represents the position vector of the non-inertia frame, $\boldsymbol{r}$ represents the radial position vector, and $\boldsymbol{\Omega}$ represents the angular velocity of rotating motion. Eq. (1), the

momentum conservation equation, is built in the MARS-KS code.

Table I: Fictitious Acceleration and Mathematical Forms [3]

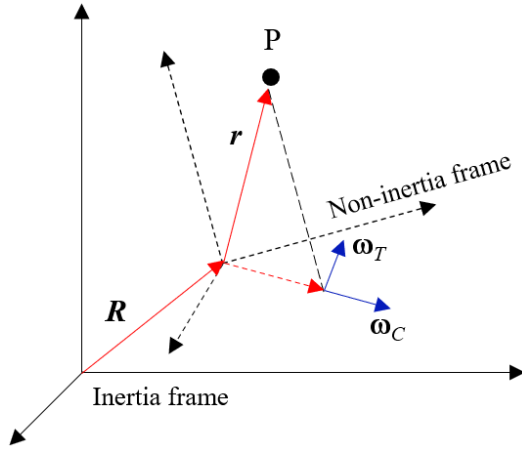| Fictitious acceleration	Mathematical form
Frame acceleration	$\dfrac{d^2 \mathbf{R}}{dt^2}$
Coriolis acceleration	$2\mathbf{\Omega} \times \mathbf{u}$
Tangential acceleration	$\dfrac{D\mathbf{\Omega}}{Dt} \times \mathbf{r}$
Centrifugal acceleration	$\mathbf{\Omega} \times (\mathbf{\Omega} \times \mathbf{r})$

Fig. 2. Centrifugal and tangential acceleration.

Fig. 2 depicts the centrifugal and tangential acceleration in each axis consisting non-inertia frame. The angular acceleration equation is expressed as summation with the centrifugal and tangential acceleration as follows:

$$\omega_{Cx} = \omega_x^2 r_x (\cos\theta_x \, \mathbf{j} + \sin\theta_x \, \mathbf{k}) \qquad (2)$$

$$\omega_{Tx} = \omega_{ax} r_x (-\sin\theta_x \, \mathbf{j} + \cos\theta_x \, \mathbf{k}) \qquad (3)$$

$$\omega_{Cy} = \omega_y^2 r_y (\cos\theta_y \, \mathbf{k} + \sin\theta_y \, \mathbf{i}) \qquad (4)$$

$$\omega_{Ty} = \omega_{ay} r_y (-\sin\theta_y \, \mathbf{k} + \cos\theta_y \, \mathbf{i}) \qquad (5)$$

$$\omega_{Cz} = \omega_z^2 r_z (\cos\theta_z \, \mathbf{i} + \sin\theta_z \, \mathbf{j}) \qquad (6)$$

$$\omega_{Tz} = \omega_{az} r_z (-\sin\theta_z \, \mathbf{i} + \cos\theta_z \, \mathbf{j}) \qquad (7)$$

$$\mathbf{a}_{angular} = \sum \omega_{Cx,y,z} + \sum \omega_{Tx,y,z} \qquad (8)$$

where θ_x, θ_y, and θ_z are rotational degrees in each of three axes, $\omega_{Cx,y,z}$ is the centrifugal acceleration of each axis, $\omega_{Tx,y,z}$ is the tangential acceleration, $\omega_{ax,y,z}$ is the angular acceleration, and $\omega_{x,y,z}$ is the angular velocity of each axis. Hence, the net acceleration due to the external forces can be written by the summation with gravity, three linear accelerations, and three angular accelerations as follows:

$$\mathbf{a}_{net} = \mathbf{a}_{linear} + \mathbf{a}_{angular} + g\mathbf{k} \qquad (9)$$

Accordingly, the net body force acceleration is indicated as a result of the dot product of the net acceleration due to the motions with the direction vector of volume. Consequently, the net body force acceleration is substituted into Eq. (1), the momentum conservation equation, to simulate three-dimensional motions.

3. Numerical Simulation

3.1 MARS-KS Code

The MARS-KS code is a safety analysis code developed by the Korea Atomic Energy Research Institute (KAERI) for numerical analysis of the transient thermal-hydraulic phenomena of nuclear power plants under postulated accident conditions. Furthermore, various ocean motions can be simulated using the dynamic motion model option built into the code. Hence, in this paper, the single-phase natural circulation performance was analyzed using the MARS-KS code with a dynamic motion model.

3.2 Simple Natural Circulation Loop

The MARS-KS code simulated thermal-hydraulic conditions for natural circulation behavior in the simple rectangular loop. The simplified one-loop design in Fig. 3 and single-phase flow were adopted to analyze the fundamental effect caused by dynamic motions on natural circulation in steady-state.
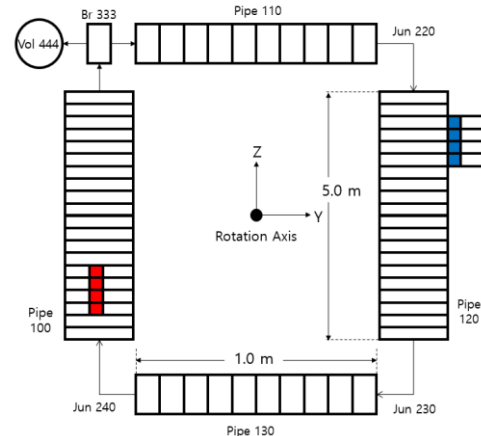

Fig. 3. MARS-KS nodalization of analytical model.

A one-dimensional loop consisted of a heater, a cooler, and pipes components. The cylindrical heater was installed inside heated pipes supplying constant heat without heat loss. The heater is the composition of UO_2 and Zr-alloy, the representative PWRs fuel, and the general reactor cladding material, respectively. The annular cooler with stainless steel was attached to the cooling pipes removing the same amount of supplied heat. Consequently, the natural circulation occurred due

to the density difference of the fluid between the heater and the cooler. The thermal-hydraulic conditions and geometrical information for analytical models are given in Fig. 3 and Table II.

4. Results and Discussion

4.1 Rolling

The rolling motion in the simple loop was imitated to 15° with a period of 12 seconds per cycle, which is the representative value of rolling degree and period in ocean environments [5], in the MARS-KS code. The mass flow rate with two cycles under this rolling condition has a sine wave shape over time.

As shown in Fig. 3, the elevation difference in the thermal centers between the heater and the cooler was initially inclined toward the heater. Hence, the mass flow rate in the test loop changed unsymmetrically with the rotating direction. The average mass flow rate under the 15° rolling condition was lower than that under the no motion condition. Therefore, the negative effect on the natural circulation of the rolling occurred despite the temporary higher mass flow rate.
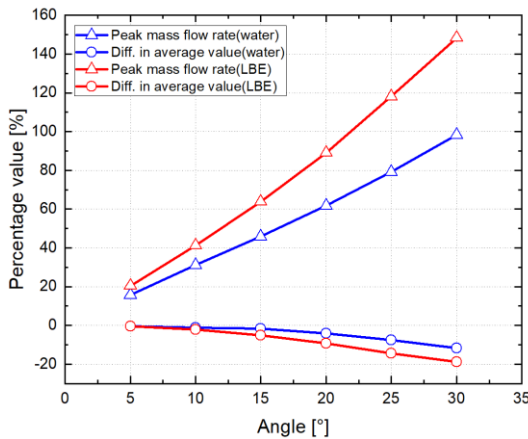

Fig. 4. Peak value and average value difference under rolling compared to no motion condition.

This behavior was identically indicated from the result of LBE. However, the difference value of LBE was higher with a 5.07% declination rate than that of water with a 1.66% declination rate. Based on this result, additional simulations were conducted varying the degree of the rolling angle at an interval of 5° from 5° to 30°. The average mass flow rate under the rolling conditions had the largest difference among the three dynamic motions compared to that with no motion, as shown in Fig. 4.

The reason for the large effect of the rolling is that the tangential forces interfere with the fluid velocity in the loop due to the parallel direction of the rolling motion concerning the loop plane. The LBE result had a larger average mass flow rate difference value than water as a working fluid because of the large tangential force due to its large density.

4.2 Pitching

The pitching motion rotating z-x plane has a well-known value in the ocean environments, 45° with 12 seconds per cycle [5]. The difference in the elevation of the thermal centers between the heater and the cooler is symmetrical regardless of the rotating direction, as inferred from Fig. 3. Therefore, the mass flow rate fluctuation had two sinusoidal cycles per single pitching period. The mass flow rate difference compared to no motion condition was 5.51% and 4.86% declination rates for LBE and water, respectively.

The additional analysis was conducted by varying the amplitude of the pitching motion at an interval of 15° from 15° to 60°. The tangential force hardly affects the fluid flow since the rotational direction was perpendicular to the loop plane. The centrifugal force was neglected since the upper and lower pipes were symmetrically located with respect to the rotational axis in the center of the loop. Consequently, there was not a higher mass flow rate than that without motion, even under the smallest pitching condition since only the elevation difference in the two thermal centers due to the pitching motion caused a negative effect on the natural circulation.

The peak mass flow rate under the pitching for both cases had the smallest value among the three motion conditions, as shown in Fig. 5. The difference in the average mass flow rate compared to the no motion condition was smaller than that under the rolling conditions. However, the LBE case had a lower peak mass flow rate than water, as opposed to the rolling conditions. In addition, the differences in the average values under the pitching motion and no motion were always higher than for LBE compared to water.

Table II: Design Parameters of Water and LBE Model

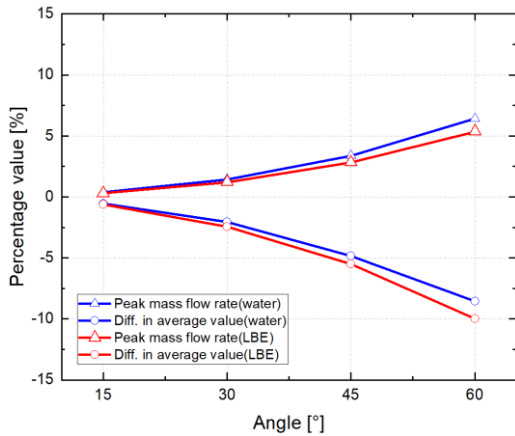| Working fluid	Light water	Lead-bismuth eutectic
Heater material	UO$_2$	UO$_2$
Cooler material	Stainless-Steel	Stainless-Steel
Cladding material	Zr-alloy	Zr-alloy
Operating pressure [MPa]	15.0	0.101
Elevation difference in the thermal centers [m]	3	3
Hydraulic diameter [mm]	19.0	19.0
Heat generation [kW]	10	30

Fig. 5. Peak value and average value difference under pitching compared to no motion condition.

4.3 Heaving

The sinusoidal wave value of heaving motion is generally known as 0.5 g with 12 seconds in the ocean [5]. The elevation difference between the heater and the cooler did not change during the heaving motion, which is dissimilar to the rolling and pitching conditions. Hence, the heaving motion increases the driving force when the direction of the heaving acceleration matches the flow direction. The mass flow rate behavior had a sinusoidal shape, similar to rolling and pitching. The average mass flow rate hardly had a variance compared to no motion condition due to symmetrical increase and decrease in the mass flow rate. The internal mass flow rate under various heaving accelerations, which are at an interval of 0.1 g from 0.1 g to 0.7 g, is represented in Fig. 6. In general, the mass flow rate behavior under the heaving was analogous to that under the rolling condition and the mass flow rate is proportional to the heaving acceleration.
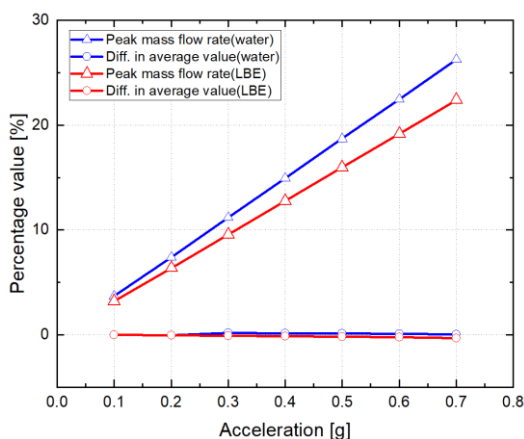

Fig. 6. Peak value and average value difference under heaving compared to no motion condition.

Peak values under heaving motions were intermediate between those under the rolling and pitching. However, the effect on the average mass flow rate is insignificant even considering the largest heaving acceleration. Consequently, the heaving motion had the most minor effect on the natural circulation among the three dynamic motion conditions.

5. Conclusions

In this study, a thermal-hydraulic behavior in the simple loop was inquired to analyze the effect of representative ocean motions on the natural circulation using the MARS-KS system code. A natural circulation behavior in the loop was similarly indicated in both working fluids, water and LBE.

The natural circulation performance decreased under rolling and pitching. The stronger dynamic motion applies, the more decrease in the mass flow rate is except the heaving conditions. The smallest effect on the average mass flow rate was indicated under the heaving condition, the largest impact was investigated under the rolling, and the pitching motion was intermediate. Consequently, careful consideration of the rolling condition than other motions is needed for designing FNPPs using natural circulation. Moreover, the installation of anti-rolling devices might be a worthwhile choice to reduce the effect of rolling, especially on nuclear-powered ships.

The peak fluctuation rate for water was lower under rolling, although the other conditions always have a higher peak value than that for LBE. Furthermore, the average mass flow rate under dynamic motion conditions always had lower difference values with no motion condition in the case of water than that of LBE because the additional acceleration for LBE is higher due to large density.

Further study on the real scaled reactor design and extreme oceanic conditions including a complex irregular motion will be required for an advanced design of FNPPs.

REFERENCES

[1] I. H. Kim, J. S. Won, T. H. Bae, K. W. Yi, H. R. Choi, G. S. Kim, S. K. Lee, S. J. Kim, C. K. Chung, B. G. Kim, J. T. Seo, and B. J. Lee, Development of BANDI-60S for a floating nuclear power plant, Fuel, Vol. 290, pp. 325, 2019.
[2] G. W. Kim, G. C. Park, and H. K. Cho, Scaling analysis for single-phase natural circulation under dynamic motion and its verification using MARS-KS code, Annals of Nuclear Energy, Vol. 159, 2021.
[3] H. K. Beom, G. W. Kim, G. C. Park, and H. K. Cho, Verification and improvement of dynamic motion model in MARS for marine reactor thermal-hydraulic analysis under ocean condition, Nuclear Engineering and Technology, Vol. 51, No. 5, pp. 1231-1240, 2019.
[4] G. L. Mesina, D. L. Aumiller, F. X. Buschman, and M. R. Kyle, Modeling moving systems with RELAP5-3D, Nuclear Science and Engineering, Vol. 182, No. 1, pp. 83-95, 2016.

[5] E. V. Lewis, The motion of ships in waves, Principles of naval architecture, 1967.